DENTAL MATERIALS 35 (2019) 1214–1226

Available online at www.sciencedirect.com

ScienceDirect

journal homepage: www.intl.elsevierhealth.com/journals/dema

Effects of HEMA on Nrf2-related gene expression using a newly developed 3D co-culture model of the oral mucosa

Renke Perduns[a,*], *Joachim Volk*[a], *Melanie Plum*[a], *Frank Gutzki*[b], *Volkhard Kaever*[b], *Werner Geurtsen*[a]

[a] *Department of Conservative Dentistry, Periodontology and Preventive Dentistry, Hannover Medical School, D-30625 Hannover, Germany*

[b] *Research Core Unit Metabolomics, Hannover Medical School, D-30625 Hannover, Germany*

ARTICLE INFO

Article history:
Received 15 February 2019
Received in revised form
26 April 2019
Accepted 7 May 2019

Keywords:
HEMA
Oral keratinocytes
Gingival fibroblasts
3D co-culture
Redox-regulated gene expression

ABSTRACT

Objective. 2-Hydroxyethyl methacrylate (HEMA) is a component of many resin-modified materials and elutes from dental restorations into the oral cavity. Objective of our investigation was to determine the impact of HEMA on oral keratinocytes (OKF6/TERT2) and gingival fibroblasts (HGFs) in a newly established 3D co-culture model (3D-CCM) and to analyze the permeability of OKF6/TERT2 cells for HEMA.

Methods. Well-characterized 3D-CCMs, consisting of confluent OKF6/TERT2 cells on cell culture inserts above HGF-containing collagen gels, were treated supra-epithelial with HEMA. Mass spectrometry was used to measure the supra- and sub-epithelial distribution of HEMA after 24 h. The impact of HEMA on nuclear factor erythroid 2-related factor 2 (Nrf2) target genes was measured by qRT-PCR and western blot analysis.

Results. Mass spectrometry showed that HEMA was evenly distributed above and below the keratinocyte layer after 24 h. Analyzed target genes of Nrf2 were induced in both cell types on the mRNA-level but less pronounced in HGFs. On the protein-level, both cell types showed similar effects: At 5 mM HEMA, heme oxygenase-1 was induced 5.1-fold in OKF6/TERT2 cells and 4.1-fold in HGFs. NAD(P)H quinone dehydrogenase-1 was approximately induced 1.85-fold in both cell types.

Significance. Our 3D-CCM is suitable to analyze the biocompatibility of dental materials due to an improved simulation of the oral mucosa compared to monolayer cultures. Our results indicate that HEMA is able to penetrate a dense layer of keratinocytes and to activate the cellular oxidative defense response. This may be due to the activation of the Nrf2-pathway in both cell types.

* *Corresponding author at*: Department of Conservative Dentistry, Periodontology and Preventive Dentistry, Hannover Medical School, Carl-Neuberg-Str. 1, D-30625 Hannover, Germany.

E-mail addresses: Perduns.Renke@MH-Hannover.de (R. Perduns), Volk.Joachim@mh-hannover.de (J. Volk), Plum.Melanie@mh-hannover.de (M. Plum), Gutzki.Frank@mh-hannover.de (F. Gutzki), Kaever.Volkhard@mh-hannover.de (V. Kaever), Geurtsen.Werner@mh-hannover.de (W. Geurtsen).

https://doi.org/10.1016/j.dental.2019.05.006

1. Introduction

Resin-based restorative materials are widely used in dentistry. Resin-modified materials are based on a radical chain polymerization of monomers, for example methacrylates like 2-hydroxethyl methacrylate (HEMA), which is triggered by initiators. Several studies have shown that unpolymerized monomers elute from the resinous matrix into the oral cavity [1,2]. To our knowledge, no studies exist that quantified the concentration of eluted HEMA *in vivo*. However, a meta-analysis of data derived from *in vitro* studies showed that 2.3 nmol of HEMA might elute per mm^3 of restoration in water-based solutions within the first 24 h [3]. These data indicate that HEMA concentrations might reach the single-digit mM range, for instance, when the restoration is located underneath the gingiva or placed after a direct pulp-capping procedure [4]. Incomplete curing could increase the concentration further.

Cytotoxic and molecular effects of HEMA have been studied in monolayers of different cell types [5,6]. HEMA causes various effects like the reduction of proliferation, modulation of the immune response caused by pathogens, or the induction of micronuclei [7–9]. These reactions have been linked to the generation of oxidative stress, which may be caused by the depletion of intracellular glutathione (GSH) by the formation of HEMA-GSH adducts [10–12]. One of the main mechanisms of cells to maintain redox homeostasis is the nuclear factor erythroid 2-related factor 2 (Nrf2) dependent signaling pathway. Nrf2 is constitutively expressed and directly degraded in the cytoplasm. When oxidative stress occurs, Nrf2 is stabilized and translocated to the nucleus where it activates the transcription of corresponding genes [13]. Additionally, it has been described that the Nrf2 promoter itself has two Nrf2-binding sites, potentially to enhance its own expression by a positive feedback loop [14,15]. Target genes of Nrf2 are, for example, heme oxygenase 1 (*HO-1*), NAD(P)H quinone dehydrogenase 1 (*NQO1*), superoxide dismutase 1 (*SOD1*), and glutathione peroxidase 4 (*GPx4*), which either directly or indirectly detoxify reactive oxygen/nitrogen species (ROS/RNS) [16–20].

Studies that analyzed the molecular effects of HEMA on different cell types used monolayer cultures. However, monolayer cultures have limitations when it comes to the in-depth analysis of molecular mechanisms and their clinical relevance. Cells grown in monolayer cultures differ in their morphology and physiology due to the lack of spatial adhesion domains and the stiffness of glass or plastic surfaces [21–23]. This leads to alterations of parameters like cell migration, cell proliferation, cell differentiation and the basal transcriptome between cells grown in monolayer cultures and cells grown in a three-dimensional (3D) environment [24–27]. Additionally, it has been shown that responses of cells grown in 3D cultures are more similar to the *in vivo* situation compared to cells grown in monolayer cultures [28,29]. Another potential limitation of conventional monolayer cultures is due to the lack of interactions with other cell types compared to the *in vivo* setting. For instance, the co-culture of fibroblasts and keratinocytes has been studied to understand the interaction between both cell types especially during the process of wound healing. It has been shown that the balance of matrix metallopeptidases (MMPs) and corresponding tissue inhibitors of metalloproteinases (TIMPs) dependents on the interaction between both cell types and differs between cell monolayers and co-cultures [30,31]. The regulation of cell migration, differentiation and proliferation of keratinocytes and fibroblasts is also regulated by complex networks of signaling molecules and paracrine growth factor loops between both cell types [32,33].

In recent years, studies have been carried out with co-culture models that incorporate 3D matrices to improve the simulation of the natural mucosa *in vitro*. In those models, keratinocytes were directly seeded on 3D scaffolds (like collagen) either without fibroblasts [34] or with fibroblasts embedded in 3D matrices to generate organotypic models of the oral mucosa [35,36]. These models have been used mainly to study host-pathogen interactions [37,38]. In 1997, Schmalz et al. analyzed the effect of metals used in dentistry on cell survival and prostaglandin E2 release in commercial 3D cell culture models [39]. But to our knowledge, the molecular interactions of composite resins regarding the regulation of genes and proteins from different cells from the oral mucosa have not yet been analyzed in 3D co-culture models.

The aim of our study was to analyze the effect of HEMA on the expression of mRNA and protein of genes related to the oxidative stress defense in a 3D co-culture model, which mimics the oral mucosa. For that, we established a co-culture model with human oral keratinocytes and collagen-embedded gingival fibroblasts of the mucosa. Both cell types were separated by a porous membrane to allow paracrine interactions between the two cell types and to allow for a separate sampling of keratinocytes and fibroblasts (Fig. 1a). We aimed to investigate whether (1) HEMA induces key enzymes of the cellular oxidative stress defense system by real time PCR and western blotting, (2) HEMA passes the *in vitro* endothelial barrier of oral keratinocytes using gas chromatography–mass spectrometry (GC/MS) and if (3) HEMA exerts similar effects on cells grown in our 3D co-culture model in comparison to cells from monolayer cultures.

2. Material and methods

2.1. Cell cultures

Cell cultures of human gingival fibroblasts (HGFs) were grown from a biopsy of the gingiva of permanent molars of a healthy patient. The tissue donor was informed and we obtained consent according to the guidelines of the Institutional Review Board. HGFs were cultivated in Dulbecco's modified Eagle's medium with 4.5 g/L glucose, 25 mM 2-[4-(2-hydroxyethyl)-1-piperazinyl] ethane sulfonic acid (HEPES), 4 mM L-glutamine, 3.7 g/L $NaHCO_3$, 100 U/mL penicillin, 100 μg/mL streptomycin and 2.5 μg/mL amphotericin B, supplemented with 10% fetal bovine serum (FBS, all from Biochrom KG, Berlin, Germany) at 37 °C and 10% CO_2 in a humidified atmosphere. Cells were supplied with fresh medium three times a week. HGFs were detached by trypsin/ethylenediaminetetraacetic acid (EDTA, 0.25% trypsin, 0.02% EDTA; GIBCO/Invitrogen, Darmstadt, Germany) and seeded in new culture flasks when the

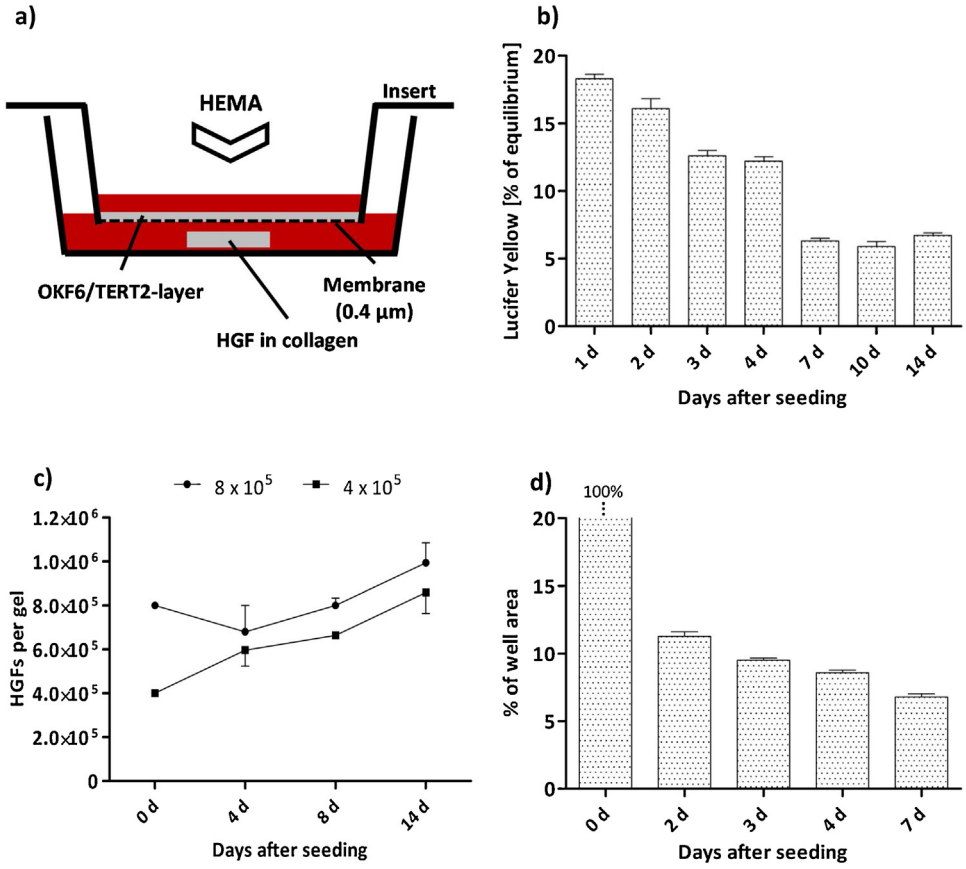

Fig. 1 – Characterization of the 3D co-culture model. (a) Schematic image of the 3D co-culture model (Red = growth medium). (b) LY retention by OKF6/TERT2 cells grown on cell culture inserts over a period of 14 d. The relative amount of LY that passed the membrane was calculated relative to the equilibrium concentration. (c) Cell numbers of HGFs grown in collagen gels. Two different concentrations of HGFs were seeded in collagen gels (indicated at 0 d). The quantity of HGFs per gel was measured following a collagenase digestion at three time points. (d) Contraction of HGF-containing collagen gels. The area of collagen gels was measured during pre-cultivation of cells and before the 3D co-culture systems were assembled. The area is shown in relation to the area of a well of 6-well plates (Y-axis). The column at the day of seeding (0 d) is capped at 20% for a clear view. (b), (c), (d) means ± SD from three independent replicates are shown. (For interpretation of the references to colour in this figure legend, the reader is referred to the web version of this article.)

confluency reached about 90%. HGFs from passages six or seven were used to set up the 3D culture in collagen gels.

The immortalized oral keratinocyte cell line OKF6/TERT2 was provided by Dr. J. Rheinwald (Havard University) [40]. OKF6/TERT2 cells were cultured in serum-free medium (ker-sfm) supplemented with 25 µg/mL bovine pituitary extract (BPE), 0.2 ng/mL epidermal growth factor (EGF, all from GIBCO/Invitrogen, Darmstadt, Germany), 0.3 mM $CaCl_2$, 100 U/mL penicillin, 100 µg/mL streptomycin and 2.5 µg/mL amphotericin B. For passaging, OKF6/TERT2 cells were detached by trypsin/EDTA solution (0.125% trypsin, 0.01% EDTA). Inactivation of trypsin was achieved by adding 1 volume of Dulbecco's modified Eagle medium/Ham's F-12 medium (DMEM/F-12, Biochrom KG, Berlin, Germany) supplemented with 10% FBS. OKF6/TERT2 cells for experiments were grown in medium with a higher nutrient concentration when a confluency of about 30% was reached (HD-ker): 1:1 mixture of DMEM/F-12 and ker-sfm supplemented with 25 µg/mL BPE, 0.2 ng/mL EGF, 0.2 mM $CaCl_2$, 0.75 mM L-glutamine, 100 U/mL penicillin, 100 µg/mL streptomycin and 2.5 µg/mL amphotericin B. OKF6/TERT2 cells were cultivated at 37 °C and 5% CO_2 in a humidified atmosphere at all stages.

2.2. 3D co-culture model

2.2.1. Preparation of collagen gels with fibroblasts

HGF-containing collagen gels were produced in two steps. First, acellular collagen gels were cast in 6-well plates. For that, the wells of 6-well plates were moistened with DMEM + 10% FBS and then 1 mL of acellular collagen mixture was added. The mixture was prepared on ice. It contained 0.27 mL distilled water, 0.14 mL FBS, 0.1 mL of 10× DMEM (Biochrom KG, Berlin, Germany), 0.1 mL L-glutamine (200 mM), 0.1 mL 10× reconstitution buffer (20 mM HEPES, 22 mg/mL sodium bicarbonate in 20 mL 0,062 M sodium hydroxide) and 0.38 mL of type 1 rat tail collagen (2 mg/mL in 0.1 % acetic acid; SERVA Electrophoresis GmbH, Heidelberg, Germany) per gel. The gels polymerized in 30 min at room temperature (RT). Afterwards, acellular gels

were covered with 3 mL of the cellular gel solution containing 4×10^5 HGFs. The mixture of the cellular collagen was also prepared on ice. It contained 0.84 mL distilled water, 0.25 mL FBS, 0.3 mL of 10× DMEM, 0.03 mL L-glutamine (200 mM), 0.3 mL 10× reconstitution buffer, 1.18 mL of type 1 rat tail collagen and 0.1 mL of HGFs in DMEM with 10% FBS per gel. Polymerization was achieved by incubating the gels for 60 min at RT. HGF-containing collagen gels were covered with 3 mL of HGF growth medium. After 24 h, the gels were contracted and mostly detached from the well. Gels that were not fully separated from the well were carefully detached manually using a small needle. HGF-containing collagen gels were cultivated at 37 °C and 10% CO_2 in a humidified atmosphere. The medium was exchanged three times a week. The contraction of HGF-containing collagen gels was measured until they were used for the co-culture models with OKF6/TERT2 cells seven days after the preparation, in order to ensure a consistent seeding and viability of gingival fibroblasts.

2.2.2. *Seeding of OKF6/TERT2 cells on cell culture inserts*

OKF6/TERT2 cells (5*10^5 cells in 1.5 mL HD-ker) were seeded on cell culture inserts for 6-well plates with a pore diameter of 0.4 μm (ThinCert 657641, Greiner-Bio-One, Kremsmuenster, Austria), seven days before the beginning of the co-culture with fibroblasts. 2.6 mL HD-ker was added to the lower compartment underneath the cell culture insert. OKF6/TERT2 cells on inserts were cultivated at 37 °C and 5% CO_2 in a humidified atmosphere. The medium was exchanged three times a week.

2.2.3. *Assembly of the 3D co-culture model*

Confluent OKF6/Tert2 cells grown on cell culture inserts and HGF-containing collagen gels were combined in a new 6-well plate. The gels were transferred with a sterile spatula and supplied with 2.6 mL of DMEM/F-12 medium supplemented with 25 μg/mL BPE, 0.2 ng/mL EGF, 0.2 mM $CaCl_2$, 1.5 mM L-glutamine, 100 U/mL penicillin, 100 μg/mL streptomycin, 2.5 μg/mL amphotericin B and 2% FBS (DF-K medium). Afterwards, the OKF6/TERT2 cells on the inserts were placed above the gels and supplied with 1.5 mL of DF-K medium with HEMA or control media as described in Section 2.4.

2.3. *Characterization of the 3D co-culture model*

2.3.1. *Lucifer Yellow assay*

The fluorescent dye Lucifer Yellow (Sigma-Aldrich, St. Louis, USA) was used to assess the permeability and confluency of oral keratinocytes on the cell culture inserts. Lucifer Yellow (LY) was prepared at a concentration of 1 mg/mL in Hanks' Balanced Salt solution (HBSS; Biochrom KG, Berlin, Germany) and diluted 1:20 in HD-ker to obtain the LY working solution. The growth medium of the inserts to be tested was removed and replaced with 2 mL HD-ker in the lower compartment and 1 mL of LY working solution in the upper compartment of the co-culture system. The LY working solution was diluted 1:3 in HD-ker to obtain the equilibrium control as reference for a maximal diffusion across the membrane of the inserts (equal distribution in upper and lower compartment). The cell culture systems and the equilibrium control were incubated for 1 h at 37 °C and 5% CO_2. Afterwards, 200 μL were taken from the lower compartment of the co-culture inserts and the equilibrium control, which were then transferred to different wells of a 96-well plate in technical duplicates. HD-ker was used as blank. The fluorescence of LY was measured with a Synergy H1 plate reader (excitation/emission wavelength = 428 nm/540 nm, BioTec, Neufahrn, Germany) and quantified in relation to the equilibrium control.

2.3.2. *Counting of HGFs from collagen gels*

HGFs were seeded at a density of 4×10^5 or 8×10^5 cells per gel and cultured as described in Section 2.2.1. The HGF-containing collagen gels were harvested 4, 8, and 14 d after seeding to count the cells. Initially, gels were washed for 10 min in 20 mL HBSS. Afterwards, collagen was digested by an incubation with collagenase type 1 (250 U/mL; ThermoFisher, Waltham, USA) in HBSS, supplemented with 3 mM $CaCl_2$, for 1 h at 37 °C and slow agitation. Isolated cells and cell aggregates were pelleted by centrifugation at 250 × *g* for 5 min. The supernatant was discarded and the pellet was resuspended in 1 mL 0.25% trypsin/0.02% EDTA solution. After incubating the gels for 10 min at 37 °C and slow agitation, remaining cell aggregates were resuspended by pipetting up and down gently. Cells were pelleted again and resuspended in 0.5 mL DMEM + 10% FBS. The isolated cells were counted using a TC20 automated cell counter (Biorad, Hercules, USA). Three independent experiments, each with two technical replicates, were carried out.

2.3.3. *Histology of HGF-containing collagen gels and OKF6/TERT2 cells on inserts*

Membranes with attached OKF6/TERT2 cells from cell culture inserts and HGF-containing collagen gels were fixated in 10% formalin solution for 24 h and automatically embedded in paraffin using an automated TP1020 tissue processor (Leica, New Boston, USA). Membranes were kept in a vertical orientation to facilitate cross sectioning. Resulting paraffin blocks were sectioned in 4 μm slices and stained with haematoxylin and eosin (H&E) for histological evaluation. The sections were examined using a DM4000 B microscope (Leica).

2.4. *HEMA treatment of 3D co-culture models*

Co-cultured cells were treated with 0.5 or 5 mM HEMA for 24 h. The co-monomer 2-hydroxyethyl methacrylate (HEMA) was provided by VOCO (Cuxhaven, Germany). 400-fold concentrated stock solutions of HEMA were prepared in ethanol. Stock solutions were freshly diluted 1:400 in DF-K medium supplemented with 2% FBS prior to each experiment to obtain the treatment solutions (5 mM and 0.5 mM HEMA). Growth medium with 0.25% ethanol (C1) and growth medium without ethanol (C2) served as controls. 2.6 mL of DF-K medium supplemented with 2% FBS was added to the lower compartment of 3D co-culture models and 1.5 mL of each treatment solution was added to the upper compartment to perform a supra-epithelial treatment.

2.5. *GC/MS measurement of HEMA in 3D co-culture models*

OKF6/TERT2 cells were seeded on cell culture inserts as described in Section 2.2.2 and treated with 5 mM HEMA or 0.25% ethanol as control (C1) as described in Section 2.4. After

24 h, 1 mL medium was taken from both compartments, briefly centrifuged and used for GC/MS measurements. Eight calibrators were prepared by diluting 5 mM HEMA stock solution consecutively 1:2 in DF-K medium with 0.25% ethanol to a concentration of 39.06 μM. HEMA was extracted by mixing 300 μL sample or calibrator with 300 μL ethyl acetate (Merck, Darmstadt, Germany), supplemented with 1.25 mM caffeine (Sigma-Aldrich, St. Louis, USA) as internal standard, for 10 min. Afterwards, 300 μL ethyl acetate was added, followed by vortexing for 2 min. The resulting mixture was centrifuged at 5445 × *g* (5 min, 4 °C). 50 μL of the resulting supernatant were transferred to an amber glass vial with inserts (f N11-1 HP; Macherey-Nagel, Düren, Germany) and diluted with 200 μL ethyl acetate. 1 μL of each extract was injected *via* a 7693 ALS Autosampler (Agilent Technologies, Santa Clara, USA) into the Agilent 7890B GC System equipped with a HP-5MS UI column, 30 m × 0.25 mm ID, 0.25 μm film thickness coupled to an Agilent 7000C GC/MS triple quadrupole mass spectrometer. Helium was used as carrier gas at a constant flow of 1.2 mL/min. Analytes were separated by applying the following temperature program: 50 °C initial temperature for 1 min followed by a temperature-ramp of 25 °C/min to 150 °C and a second ramp of 15 °C/min to 300 °C, held for 1 min. Under these conditions, the retention time of HEMA on the column was 3.83 min. HEMA was identified by MS *via* its m/z 69.1 and m/z 86.9 mass fragments. Experiments were repeated three times independently.

2.6. Gene expression analysis

After treatment, total RNA of both cell types was isolated. OKF6/TERT2 cells were washed with PBS and RNA was isolated using the RNeasy Plant Mini Kit (Qiagen, Hilden, Germany) according to the manual including a DNA digestion step (DNase Set, Qiagen, Hilden, Germany). HGF-containing collagen gels were shock frozen in liquid nitrogen and stored at −80 °C. Frozen gels were dissolved in 1 mL Tri Reagent (Sigma-Aldrich, St. Louis, USA) by shaking for 15 min at RT. 200 μL chloroform was added and the mixture was vortexed for 2 min followed by an incubation step for 5 min at RT. Afterwards, samples were centrifuged for 15 min at 12,000 × g and 4 °C. The aqueous phase was transferred to a new tube and washed with 1 volume chloroform (vortex, incubation, and centrifugation as above). The aqueous phase was again transferred to a new tube and total RNA was precipitated using 2 volumes of ice cold ethanol followed by an incubation step at −20 °C overnight. The next day, RNA was pelleted by a centrifugation for 20 min at 14,000 × *g* and 4 °C. Afterwards the pellet was washed with 500 μL 70% ethanol and centrifuged for 10 min at 14,000 × *g* and 4 °C. The supernatant was removed and the pellet was dried at room temperature. The RNA pellet was dissolved in 30 μL RNase and DNase free water. The concentration and 260 nm/280 nm ratio of eluted RNA from both cell types was measured with a Synergy H1 plate reader using a Take3 micro-volume plate (BioTek, Winooski, USA). The integrity of RNA was checked by agarose gel electrophoresis. 1 μg of total RNA was used for cDNA synthesis using the QuantiTect Reverse Transcription Kit (Qiagen, Hilden, Germany). cDNA synthesis was carried out according to the manual. Experiments were repeated three times independently.

2.6.1. Quantitative reverse-transcription polymerase chain reaction

Quantitative analysis of gene expression was carried out by quantitative reverse transcription PCR (qRT-PCR) using the Rotor-Gene Q system (Qiagen, Hilden, Germany). SYBR® Premix Ex Taq Kits (Takara, Kusatsu, Japan) and QuantiTect Primer Assays (Qiagen, Hilden, Germany) were used to set up the qRT-PCR reactions. The cycling conditions were an initial denaturation step of 95 °C for 30 s, followed by 40 cycles of 5 s at 95 °C for denaturation and 60 °C for 20 s for primer annealing and extension. The specificity of reactions was controlled by standard melting curves. qRT-PCRs were carried out in technical duplicates. Average PCR amplification efficiencies and ct values were calculated using LinRegPCR [41]. The gene expression was calculated relative to the two most stable housekeeping genes, identified by geNorm from six candidate housekeeping genes (18S ribosomal RNA [*18S rRNA*], Actin beta [*ACTB*], Beta-2-microglobulin [*B2M*], Glyceraldehyde-3-phosphate dehydrogenase [*GAPDH*], Succinate dehydrogenase complex subunit A flavoprotein [*SDHA*] and Tyrosine 3-monooxygenase/tryptophan 5-monooxygenase activation protein zeta [*YWHAZ*]) [42]. Housekeeping genes were identified for both cell lines independently: *SDHA* and *YWHAZ* for OKF6/TERT2 cells and *B2M* and *SDHA* for HGFs. The applied primer assays are described in previous studies from our group, except for *GPx4* (QT00067165; Qiagen, Hilden, Germany) [43,44]. Normalized ratios between the untreated control (C2) and treated samples were calculated according to the efficiency adjusted delta delta ct method [45].

2.7. Western blot

Experiments for the analysis of protein expression and mRNA abundances were executed in parallel. To isolate total cellular protein, oral keratinocytes were incubated with 1 mL 150 mM NaCl, 0.4 mM Na_3VO_4 and 0.4 mM EDTA in PBS for 5 min, scratched from the membrane of cell culture inserts and pelleted by a centrifugation for 30 s at 12,000 × *g*. HGF-containing collagen gels were shock frozen in liquid nitrogen and ground under strict cold conditions. Samples were transferred to a new 1.5 mL tube. Protein from both cell types was isolated by adding 100 μL lysis buffer (150 mM NaCl, 1 mM Na_3VO_4, 5 mM EDTA, 50 mM Tris-HCL, 0.5% Triton X-100 and a protease inhibitor cocktail: Complete, Roche, Mannheim, Germany) to the pellet of OKF6/TERT2 cells or the HGF-containing powder followed by vigorous mixing. The mixture was incubated on ice for 15 min and centrifuged for 5 min at 12,000 × *g* to pellet cell debris. The protein-containing supernatant was used for protein analysis. Protein concentration was assessed using a Pierce BCA protein assay kit (ThermoFisher, Waltham, USA) according to the manufacturer's instructions. Equal amounts of protein per sample were loaded on 12–15% sodium dodecyl sulfate (SDS) polyacrylamide gels and separated by electrophoresis (SDS-PAGE) using a Tris-glycine running buffer (1.9 M glycine, 250 mM Tris and 1% SDS). Afterwards, proteins were transferred onto a polyvinylidene difluoride membrane (PVDF, Millipore, Burlington, USA) at 240 mA for 1.5 h on ice using a wet blot system (Hoefer, Holliston, USA) with a transfer buffer consisting of 25 mM Tris, 192 mM glycine and 20% methanol. Membranes

were blocked overnight at 4 °C with 3% BSA in PBS and then incubated for 1 h with the following primary antibodies diluted in 0.5% milk powder in PBS with 0.05% Tween 20 (PBS-T): anti GAPDH (rabbit; 1:10,000; Sigma-Aldrich, St. Louis, USA), anti HO-1 (rabbit; 1:2000; Enzo Life Sciences; Farmingdale, USA) and anti NQO1 (goat; 1:1000; Abcam, Cambridge, UK). Membranes were washed with PBS-T and incubated for 1 h with the respective secondary goat anti-rabbit or rabbit anti-goat antibody conjugated with horseradish peroxidase (DakoCytomation, Hamburg, Germany) diluted 1:10,000 in PBS-T containing 0.5% milk powder. Membranes were washed again with PBS-T and developed with an enhanced chemiluminescence substrate (SuperSignal West Pico chemiluminescent substrate, ThermoFisher, Waltham, USA) using an imaging system (Fusion SL-4-400WL, Vilber, Eberhardzell, Germany). Chemiluminescence signals were quantified using Bio1D (Vilber). Experiments were carried out three times independently.

2.8. Statistics

Data were calculated relative to untreated controls (C2) and are expressed as means ± SD. Significance levels of qRT-qPCR and western blot analysis were calculated relative to respective solvent controls (C1) using one way ANOVA. The normalized fold changes of both analyses were log2 transformed to enable statistical testing. In all cases Dunnett's *post-hoc* tests were carried out to account for multiple testing.

3. Results

3.1. Characterization of the 3D co-culture models

LY assays were used to assess the permeability of the OKF6/TERT2 layer grown on cell culture inserts (Fig. 1b). LY experiments were conducted for 14 days to evaluate the progression of the permeability. A prerequisite for starting experiments with the 3D co-culture model was a constant and maximum LY retention by the keratinocyte layer to ensure cellular confluency. The amount of LY that passed through the layer of OKF6/TERT2 cells decreased continuously within the first four days after seeding from 18.3% ± 0.6% of the equilibrium concentration to 12.2% ± 0.6%. Thereafter, it remained stable at approximately 6.5% of the equilibrium concentration from day seven until day 14 after seeding.

We counted the number of HGFs from collagen gels at three time points after seeding (4 d, 8 d, 14 d) to compare the proliferation of two different seeded fibroblast quantities (Fig. 1c). The cell number slightly decreased initially to 6.8×10^5 HGFs with a SD of $\pm 1.2 \times 10^5$ after four days of culture, when 8×10^5 HGFs were seeded per gel. Afterwards, the cell number increased to approximately 1×10^6 HGFs after 14 days of culture. Starting with 4×10^5 HGFs per gel led to a more pronounced increase of the cell number. 6.0×10^5 HGFs per gel were counted after four days and the initial cell number was more than doubled after 14 days with approximately 8.6×10^5 HGFs per gel. The area of the collagen gels with the embedded gingival fibroblasts was measured within the pre-cultivation period until the 3D co-culture models were assembled (Fig. 1d). Determination of this viability marker for gel-embedded fibroblasts ensures reproducible experiments. Some HGF-containing collagen gels were still attached to the well one day after seeding. Therefore the area of the gels could not be measured with absolute precision. The area of the gels markedly decreased from 100% of the well to 11.3% ± 0.6% at the second day after seeding. From day two onwards, the area decreased slightly but consistently to 6.8% ± 0.4% of the well area seven days after seeding.

The morphology of OKF6/TERT2 cells on cell culture inserts and HGFs embedded in collagen gels was continuously documented by microscopy and additionally by hematoxylin and eosin (H&E) staining of paraffin sections before the assembly of the 3D co-culture systems, seven days after seeding (Fig. 2). OKF6/TERT2 cells formed a dense layer on the cell culture inserts as shown in Fig. 2a. Cross sections of paraffin embedded membranes from cell culture inserts showed that nuclei of OKF6/TERT2 cells were partially located on top of each other (Fig. 2b). Gingival fibroblasts migrated from collagen gels starting on day four after seeding and adhered to the bottom of the wells as shown in Fig. 2c. Fig. 2d shows that HGFs were evenly distributed in the center of collagen gels. The HGF-containing part of collagen gels was prepared on an acellular gel that did not shrink initially, which resulted in a larger sphere of the acellular part underneath the cellular part of collagen gels. HGFs continuously migrated into this originally acellular part revealing a 'filamentous' shape as shown in Fig. 2e. Fig. 2f documents the transition from the part of collagen gels that was initially acellular with fewer nuclei to the cellular part with a cell density comparable to the image in Fig. 2d. Due to these results, the HEMA experiments were started at day 7 after setting up the pre-culture.

3.2. GC/MS analysis of the HEMA distribution within the 3D co-culture models

We measured the concentration of HEMA in the upper and lower compartment of 3D co-culture models that were treated with 1.5 mL of 5 mM HEMA, applied only in the upper compartment ('supra-epithelial treatment'), for 24 h. We observed that the HEMA concentrations in both compartments reached equal concentrations of approx. 1.4 mM after 24 h. For determination of the HEMA recovery rate, we calculated the amount of HEMA molecules in 1.5 mL treatment solution of 5 mM HEMA. Considering the volume and the concentration, a resulting amount of 7.5 μmol HEMA was applied. We could recover 27.9% ± 1.1% of HEMA molecules in the upper compartment (1394 ± 56 μM or 2.091 ± 3 μmol molecules in 1.5 mL) and 48.4% ± 1.6% in the lower compartment (1452 ± 45 μM or 3.775 ± 6 μmol molecules in 2.6 mL). Accordingly, 77.3% ± 2.6% of the applied HEMA could be recovered in total. Additionally, we incubated aliquots of the 5 mM HEMA treatment solution for 24 h in a 6-well plate at 37 °C to assess the influence of the culturing conditions over 24 h on the stability of HEMA. We could recover 98.1% ± 4.5% of the initial amount of HEMA in these retained samples (data not shown).

3.3. Gene expression analysis

We analyzed the transcription of five genes (*Nrf2, HO-1, NQO1, SOD1, GPx4*), that are primarily linked to the cells' defense

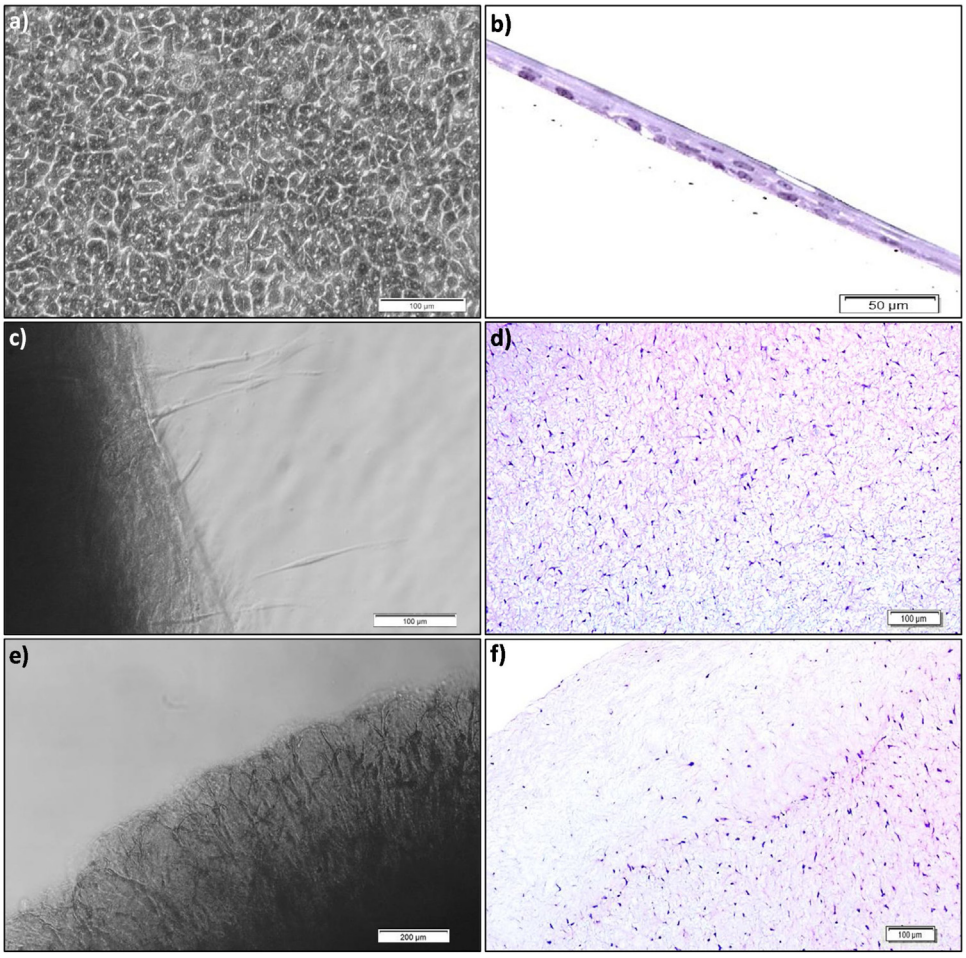

Fig. 2 – Characterization of OKF6/TERT2 cells on cell culture inserts and HGF-containing collagen gels 7 days after seeding. (a) Top view of OKF6/TERT2 cells on cell culture inserts (100× magnification). (b) H&E staining of paraffin cross sections of OKF6/TERT2 cells on cell culture inserts. (c) HGFs migrating from collagen gels (100× magnification). (d) H&E staining of paraffin sections from the center of a collagen gel. (e) HGFs at the edge of a collagen gel (40× magnification). (f) H&E staining of paraffin sections from the transition of the part of the gel that was initially acellular (upper left area) to the cellular part of collagen gels (lower right area).

against oxidative stress, after HEMA treatment with two different concentrations (5 mM and 0.5 mM HEMA; Fig. 3a). The transcription of genes was analyzed in both cell types separately 24 h after the beginning of the treatment. The transcription factor *Nrf2* was not significantly regulated in both cell types on the transcriptional level. The transcription of *HO-1* was induced by a factor of 6.3 ± 3.0 relative to the untreated control in oral keratinocytes and 6.3 ± 2.3 in gingival fibroblasts when 5 mM HEMA was applied. The abundance of *NQO1* mRNA was significantly increased at 5 mM and 0.5 HEMA in both cell types. OKF6/TERT2 cells showed an induction up to 14.3 ± 1.7 relative to the untreated control at 5 mM and 3.1 ± 1.3 at 0.5 mM HEMA. In HGFs, *NQO1* transcription was induced up to 4.4 ± 0.3 relative to the untreated control at 5 mM and 1.7 ± 0.4 at 0.5 mM HEMA. The transcription of *SOD1* and *GPx4* was not significantly affected in human gingival fibroblasts while both genes were transcriptionally induced at 5 mM HEMA in oral keratinocytes. *SOD1* was induced by a factor of 2.1 ± 0.3 and *GPx4* by a factor of 2.1 ± 0.5 relative to the untreated control. Interestingly, *NQO1* showed the tendency for a more pronounced increase in OKF6/TERT2 cells compared to HGFs. *SOD1* and *GPx4* were induced in oral keratinocytes only.

3.4. *Western blot analysis*

We analyzed the influence of 0.5 mM and 5 mM HEMA on the expression of two proteins associated with the cellular defense against oxidative stress (HO-1 and NQO1). Fig. 4a shows the averaged results of the quantification of signals from western blots of three independent experiments. HO-1 was significantly induced by a factor of 5.1 ± 2.2 compared to the untreated control in OKF6/TERT2 cells and by a factor of 4.1 ± 0.5 in HGFs, when 5 mM HEMA was applied. In HGFs, 0.5 mM HEMA also caused a slight but significant induction of HO-1 protein by 1.3 ± 0.2 compared to the untreated control. The protein content of NQO1 was induced at 5 mM HEMA in both cell types. In oral keratinocytes NQO1 was induced

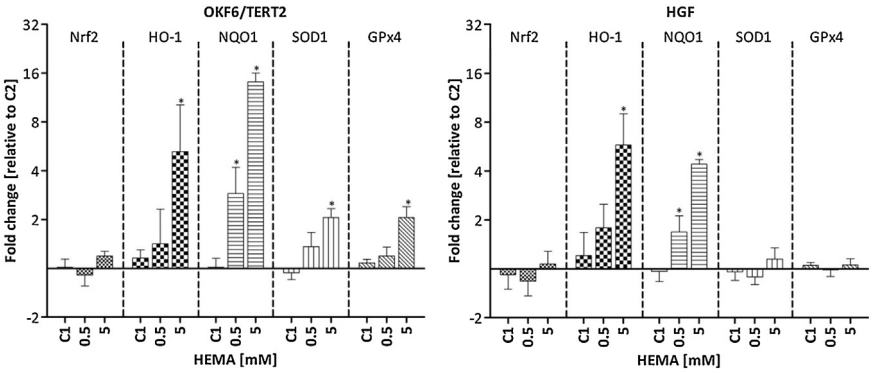

Fig. 3 – HEMA-induced alterations of the transcription of genes related to oxidative stress in HGFs and OKF6/TERT2 cells from 3D co-culture models. 3D co-culture models were treated with the indicated concentrations of HEMA for 24 h. Gene expression was analyzed by qRT-PCR and normalized to the expression of two stable reference genes (OKF6/TERT2: SDHA and YWHAZ, HGF: B2M and SDHA). The data are shown as means from three biological replicates ± SD of log2-transformed fold changes relative to untreated medium control (C2). For a better clearness, log2 values at the Y-axis were transformed to linear values. Asterisks above the error bars indicate significant differences ($P < 0.05$) in comparison to the corresponding solvent control C1 (0.25% EtOH; ANOVA, Dunnett's post-hoc test).

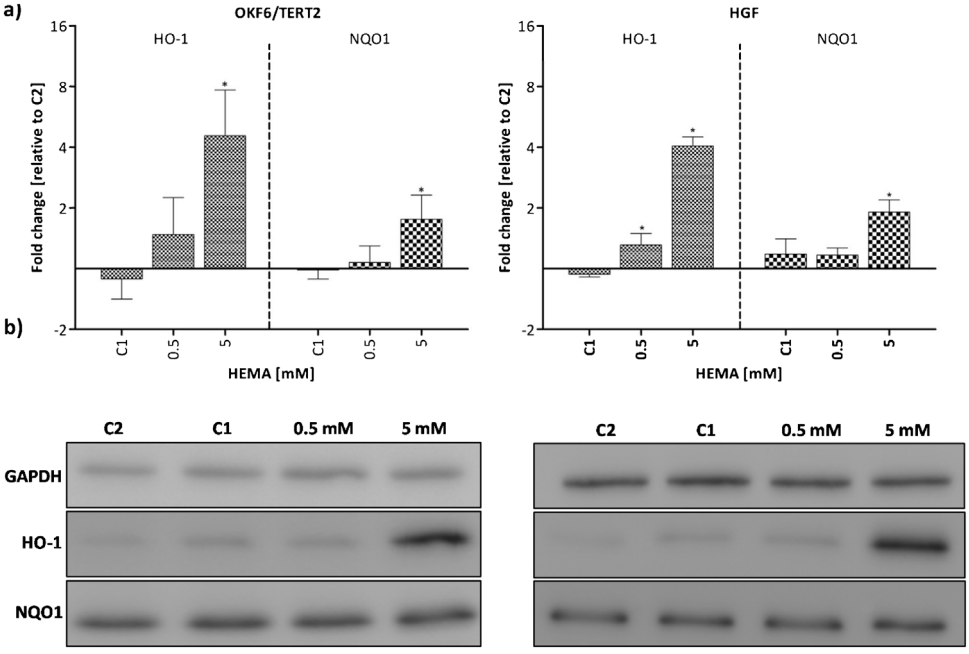

Fig. 4 – HEMA-induced alterations in protein expression of OKF6/TERT2 cells and HGFs in 3D co-culture models. 3D co-culture models were treated with the indicated concentrations of HEMA for 24 h. Protein amounts were analyzed by western blots in three biological replicates. Amount of loaded total protein per sample: GAPDH: 2.5 μg, HO-1: 5 μg and NQO1: 5 μg. (a) Chemiluminescence signals were quantified by Bio1D. Protein abundances from HO-1 and NQO1 were normalized to GAPDH as housekeeping gene and are shown as means ± SD of log2-transformed fold changes relative to the untreated medium control (C2). Log2 values at the Y-axis were transformed to linear values. Asterisks above the error bars indicate significant differences ($P < 0.05$) in comparison to the according solvent control C1 (0.25% EtOH; ANOVA, Dunnett's post-hoc test). (b) Representative western blots of all analyzed proteins.

1.8 ± 0.4-fold compared to the untreated control and in human gingival fibroblasts by a factor of 1.9 ± 0.3 when cells were treated with 5 mM HEMA for 24 h. GAPDH was used as an internal control and showed steady expression over all samples as shown by representative blots in Fig. 4b.

4. Discussion

In the present study, we used a newly developed 3D co-culture model, to analyze the effects of the resin monomer HEMA on the redox-regulated mRNA/protein expression.

Mass spectrometry-based measurements showed that HEMA molecules passed the confluent keratinocyte layer and reached the underlying fibroblasts. qRT-PCR and western blot analyzes revealed that important enzymes related to the cellular defense against oxidative stress were induced on the protein and mRNA level.

Oral keratinocytes and gingival fibroblasts are one of the first target cells of components released from dental resins. To establish an appropriate *in vitro* test system, that mimics an *in vivo*-like environment, which consists of human oral mucosa, we generated a 3D co-culture model by seeding immortalized keratinocytes onto membranes with a pore diameter of 0.4 μm on top of primary fibroblasts embedded in a collagen I scaffold (Fig. 1a). This setting enables paracrine interactions between keratinocytes and fibroblasts and still allows for a separate sampling of both cell types. We characterized the model by different methods and showed that OFK6/TERT2 cells grew as dense layer and that HGFs were distributed throughout the collagen matrix, altered the extracellular matrix (ECM) and migrated within the gel.

The LY assay is mainly used to evaluate paracellular transport, which refers to the transfer of molecules across an epithelium by passing through the intercellular space between cells [46,47]. We applied LY to analyze the permeability of the keratinocyte layer and thus to define a reproducible integrity marker of the keratinocytes barrier representing the degree of confluence of oral keratinocytes seeded on cell culture inserts. We observed a continuous decrease of LY that passed the layer of OKF6/TERT2 cells until 7 d after seeding followed by a steady plateau phase of approximately 6.5% of the equilibrium concentration until the end of experiments (14 d). Our data indicate that the OKF6/TERT2 layers reached the minimal permeability 7 d after seeding, when we started the HEMA treatment (Fig. 1b). Microscopic images and H&E stained samples of OKF6/TERT2 cells on culture inserts are in accordance with the results from the LY assay and show a very dense layer 7 d after seeding with partially stacked nuclei. We conducted LY assays in every experiment 7 days after seeding to ensure that the desired permeability of OKF6/TERT2 cells was reached before the HEMA-treatment. The threshold for maximal confluence and minimal permeability was defined as 8% LY of the equilibrium concentration.

We seeded two different concentrations of HGFs (4×10^5 and 8×10^5) in collagen gels and analyzed the development of the cell number as an indicator for cell proliferation and thus as a parameter for cell viability (Fig. 1c). The cell number increased slowly from both seeded starting quantities and converged at the end of the experiments. A tendency for a slight drop in comparison to the seeded cell number was observed 4 d after seeding when a concentration of 8×10^5 HGFs was used. This may be explained by two possibilities: Either some of the seeded cells died within the first 4 days or the cell number was underestimated due to a loss of a certain share of the cells during the time-consuming procedure of the collagenase digestion, which included two centrifugation steps. However, the measurement was reproducible as indicated by rather small standard deviations. This clearly implies that the HGFs proliferated in the collagen gels, especially when 4×10^5 cells were seeded, although the volume of the collagen gels decreased continuously. It has been described previously that the proliferation of HGFs in collagen gels is lower in comparison to monolayer cultures [30]. This effect seems to be associated with different attachment tensions of the cells with the substrates, either stiff plastic surfaces or flexible 3D matrices [48]. For experiments including HEMA-treatments, 4×10^5 HGFs were seeded per gel to allow for a proliferation and to avoid an excess of cells at early stages.

The contraction of HGF-containing collagen gels is another indicator for the viability and functionality of HGFs growing in collagen gels (Fig. 1d). Fibroblasts from different sources contract floating collagen gels through the processing of loose collagen fibrils to a more compact configuration, which leads to the exclusion of water [49]. This process is influenced by various factors, like growth factors and mechanical stimuli. It is potentially used to maintain tensional homeostasis [50,51]. Microscopic images of H&E stained samples of HGF-containing collagen gels showed that HGFs were evenly distributed throughout the cellular part of collagen gels (Fig. 2d). HGFs migrated into the part of collagen gels that was initially acellular and also out of the collagen gels where HGFs adhered to the plastic surface (Fig. 2c, e and f). Cell migration within 3D matrices is highly complex and not yet fully understood. Factors like pore size and stiffness of the matrix regulate cell migration as well as the thickness and alignment of fibers [52,53]. Additionally, high cell densities lead to enhanced cell migration especially in 3D matrices, which may explain the migration of HGFs into the acellular part and out of the collagen gels [54]. Taken together, the characterization of the 3D co-culture model showed that OKF6/TERT2 cells grow as dense layer (Fig. 2a and b). Furthermore, HGFs in collagen gels were viable as indicated by proliferation, migration and processing of the collagen matrix.

The purpose of the 3D co-culture model is to improve the clinical relevance of biocompatibility analyzes of dental materials *in vitro* in comparison to monolayer cultures by getting closer to the *in vivo* situation. We used a supra-epithelial treatment of 3D co-cultures with two different HEMA concentrations (5 mM and 0.5 mM). Thus, keratinocytes were exposed to HEMA before HGFs, like *in vivo*, in the presence of a healthy oral mucosa. We measured the amount of HEMA that passed through confluent keratinocytes to determine the permeability of OKF6/TERT2 layer for HEMA and thus to determine the HEMA concentration the gingival fibroblast were exposed to after 24 h (Table 1). It has been described previously that HEMA is able to diffuse through the dentin barrier and to reach the pulp due to its comparatively high hydrophilicity and its low molecular weight (130.4 Da) [55,56]. But so far, it has not been investigated if HEMA is able to pass a cell layer of oral keratinocytes. Our analysis showed that HEMA is evenly distributed between the upper and lower compartment of the 3D co-culture model after 24 h. This indicates that HEMA can readily pass a confluent cell layer *in vitro*. HEMA may either pass the cell layer directly through the cells (transcellular) or through the spaces between the cells (paracellular) to reach the lower compartment. In our experiments, LY was able to penetrate keratinocyte layers to some degree within one hour. LY is a hydrophilic molecule, which cannot penetrate cell membranes. Therefore, it is used to analyze the paracellular transport. HEMA could take the same route like LY to some extent, although oral keratinocytes form a dense

Table 1 – Mass spectrometry-based measurement of HEMA in 3D co-culture models.

Compartment	Vol.	HEMA applied	Conc. after 24 h	Amount of HEMA	Recovered
Upper	1.5 mL	5000 μM (7.5 μmol)	1394 ± 56 μM	2.091 ± 3 μmol	27.9 ± 1.1%
Lower	2.6 mL	x	1452 ± 45 μM	3.775 ± 6 μmol	48.4 ± 1.6%
				Total	77.3 ± 2.6%

cell layer with tight junctions to enforce cell–cell contacts [57]. It was shown as well that C^{14}-labeled HEMA, its metabolized products and also GSH-HEMA conjugates were found intracellularly [58,59]. This indicates that HEMA can pass membranes to some extent. Additionally, it is likely that HEMA has to enter the cells to cause molecular effects and to modulate the metabolism, like the induction of oxidative stress, either by diffusing through the plasma membrane or by an unspecific transport. This assumption is supported by the observation that HEMA modulates the immune status of spleen cells in mice following a topical application of HEMA [60]. In addition, our GC/MS results showed that only a certain share of the applied HEMA could be recovered in the 3D co-culture model (Table 1). However, we could retrieve a considerably higher amount of HEMA in aliquots of the treatment solution control (without cells) that were incubated for 24 h at 37 °C. This indicates that HEMA is stable in growth medium at 37 °C at least for 24 h. Our results imply that a fraction of the HEMA was metabolized in the presence of cells and, therefore, was not detectable in GC/MS readings due to the resulting shift of the molecular mass and/or due to its accumulation in cells. Three ways for the metabolism of HEMA have been described so far: Once HEMA reaches the cytoplasm it is either directly hydrolyzed to methacrylic acid by cellular esterases, or it binds lysine residues of proteins or thiol groups of reduced GSH [58,11,61]. Taken together, the GC/MS results showed that a certain share of the applied HEMA is potentially metabolized in cells. Furthermore, HEMA is obviously able to penetrate a dense layer of oral keratinocytes.

We analyzed effects caused by HEMA in the 3D co-culture model on the transcription of five genes, which are associated with the cells' defense against oxidative stress (*Nrf2, HO-1, NQO1, SOD1* and *GPx4*; Fig. 3). Two of these genes (*HO-1* and *NQO1*) were also analyzed on the protein level (Fig. 4). Except for *Nrf2*, all analyzed genes (*HO-1, NQO1, SOD1* and *GPx4*) were transcriptionally induced in OKF6/TERT2 cells, whereas only the mRNA levels of *HO-1* and *NQO1* were significantly increased in collagen-embedded HGFs. On the protein level, HO-1 and NQO1 were also induced in both cell types, which, to our knowledge, is shown for the first time for human oral keratinocytes and gingival fibroblasts. The induction of four analyzed target genes of Nrf2 on the mRNA level and two on the protein level indicates that the Nrf2 signaling pathway was activated. SOD1 is specifically detoxifying superoxide anions and produces hydrogen peroxide [18]. GPx4 detoxifies lipid peroxides in the presence of reduced thiols, even within membranes or lipoproteins [62]. Lipid peroxides are a possible consequence of the generation of superoxide anions through the oxidation of lipids [63]. NQO1 also detoxifies superoxide anions directly. In addition, it provides protection against membrane peroxidation *via* the reduction of hydrophobic antioxidants, like co-enzyme Q [16]. HO-1 produces biliverdin, which is converted to bilirubin. Both molecules detoxify a broad spectrum of ROS and RNS like hydrogen peroxide, lipid hydroperoxides and peroxynitrite [64,65]. Taken together, our results indicate that oxidative stress was induced, potentially caused by the depletion of intracellular GSH by HEMA as described previously [11,12]. Furthermore, the transcriptional induction of *SOD1* implies that superoxide was generated among other ROS/RNS.

The induction of genes associated with the defense against oxidative stress was more pronounced in OKF6/TERT2 cells compared to HGFs as described above. The different effects of HEMA on the two cell types may be due to the facts, that, firstly, keratinocytes and fibroblasts react differently to equivalent HEMA concentrations [6,43]. Secondly, HEMA was applied only in the upper compartment of the 3D co-culture model. OKF6/TERT2 cells on cell culture inserts were exposed to 5 mM or 0.5 mM HEMA directly after the application. Over time, HEMA was continuously diluted because of the distribution into the lower compartment until the equilibrium concentration (maximal: 1.83 mM or 0.183 mM) was reached. *Vice versa*, the exposition of HGFs to HEMA was delayed in the lower compartment and the concentration was lower. Interestingly, even 0.183 mM HEMA seemed to be sufficient to significantly induce the transcription of *NQO1* and to increase the protein content of HO-1 in HGFs. All analyzed genes are target genes of the transcription factor Nrf2 [17,20]. We previously reported a slight but significant increase in *Nrf2* transcription, when OKF6/TERT2 cells in monolayer culture were treated with 10 mM or 5 mM HEMA for 24 h. This increase was associated with a strong induction of *HO-1* transcription of more than 35-fold in comparison to the untreated controls [43]. In the 3D co-culture model, the level of *HO-1* mRNA was increased approximately 6.3 fold. But *Nrf2* transcription was not induced significantly. On the contrary, *NQO1* transcription showed a more pronounced increase in OKF6/TERT2 cells in the 3D co-culture model (14.3 fold) in comparison to monolayer cultures (8.6 fold), when cultures were treated with 5 mM HEMA. Additionally, the induction of *SOD1* did not differ significantly between both culture types [43]. Although *HO-1*, *NQO1* and *SOD1* share some properties regarding their role and their regulation by Nrf2, they are regulated by different transcription factors. For example, the transcription factors HIf-1α and AP-1 are involved in the ethanol-dependent induction of *HO-1*, while they do not participate in the induction of *NQO1* [66]. The promoter of *SOD1* has a binding site for AP-1 but not for HIf-1α [67]. Therefore, the observed differences between the 3D co-culture model and the monolayer cultures are potentially based on general differences regarding the basal transcriptomes, proteomes and phosphoproteomes as described previously [68,29]. It is likely that these differences influence and modulate the magnitude of stress responses against oxidative stress.

Our results showed that HEMA induces gene and protein expression of components of the cellular defense machin-

ery against oxidative stress in directly exposed human keratinocytes in the upper compartment, and gingival fibroblasts in the lower compartment of the 3D co-culture. HEMA is obviously able to penetrate a dense layer of oral keratinocytes, either by paracellular or by transcellular transport. There have been concerns regarding the clinical relevance of results, which were generated in experiments with monolayer cell cultures. These concerns specifically addressed the effects caused by dental materials on cellular metabolism in monolayer cultures. The HEMA-dependent induction of mechanisms on the mRNA- and protein-level, which we documented in our 3D co-culture model were different from those observed in monolayer cultures. Although cells of the same type and origin were used in both culture systems, the relative 'magnitudes' of effects were different. However the quality of the effects was equivalent. These documented differences may be explained by the alteration of the gene and protein expression caused by the 'cross-talk' between both cell types and their growth in different spatial environments [69,30,68]. In conclusion, our data show that the presented 3D co-culture model may be of high value for a more "*in vivo*-like" preclinical assessment of the biocompatibility of dental materials and their components. Therefore, it should help to improve the risk assessment of these materials due to a better simulation of the natural mucosa *in vitro*.

Acknowledgements

Our thanks are due to Ms. S. Wielgosz and Ms. A. Beckedorf for their commitment and excellent technical assistance. Furthermore we would like to thank Dr. Kampmann and Ms. S. Rausch for their support regarding the histological methods. This study was supported by a grant of the Deutsche Forschungsgemeinschaft/German National Science Foundation (DFG) (VO 1727/1-4).

REFERENCES

[1] Furche S, Hickel R, Reichl FX, van Landuyt K, Shehata M, Durner J. Quantification of elutable substances from methacrylate based sealers and their cytotoxicity effect on with human gingival fibroblasts. Dent Mater 2013;29:618–25.
[2] Michelsen VB, Moe G, Strøm MB, Jensen E, Lygre H. Quantitative analysis of TEGDMA and HEMA eluted into saliva from two dental composites by use of GC/MS and tailor-made internal standards. Dent Mater 2008;24:724–31.
[3] van Landuyt KL, Nawrot T, Geebelen B, De Munck J, Snauwaert J, Yoshihara K, et al. How much do resin-based dental materials release? A meta-analytical approach. Dent Mater 2011;27:723–47.
[4] Noda M, Wataha JC, Kaga M, Lockwood PE, Volkmann KR, Sano H. Components of dentinal adhesives modulate heat shock protein 72 expression in heat-stressed THP-1 human monocytes at sublethal concentrations. J Dent Res 2002;81:265–9.
[5] Bakopoulou A, Papadopoulos T, Garefis P. Molecular toxicology of substances released from resin-based dental restorative materials. Int J Mol Sci 2009;10:3861–99.
[6] Geurtsen W, Lehmann F, Spahl W, Leyhausen G. Cytotoxicity of 35 dental resin composite monomers/additives in permanent 3T3 and three human primary fibroblast cultures. J Biomed Mater Res 1998;41:474–80.
[7] Chang H-H, Guo M-K, Kasten FH, Chang M-C, Huang G-F, Wang Y-L, et al. Stimulation of glutathione depletion, ROS production and cell cycle arrest of dental pulp cells and gingival epithelial cells by HEMA. Biomaterials 2005;26:745–53.
[8] Di Nisio C, Zara S, Cataldi A, Di Giacomo V. 2-Hydroxyethyl methacrylate inflammatory effects in human gingival fibroblasts. Int Endod J 2013;46:466–76.
[9] Schweikl H, Schmalz G, Spruss T. The induction of micronuclei in vitro by unpolymerized resin monomers. J Dent Res 2001;80:1615–20.
[10] Gallorini M, Petzel C, Bolay C, Hiller K-A, Cataldi A, Buchalla W, et al. Activation of the Nrf2-regulated antioxidant cell response inhibits HEMA-induced oxidative stress and supports cell viability. Biomaterials 2015;56:114–28.
[11] Samuelsen JT, Kopperud HM, Holme JA, Dragland IS, Christensen T, Dahl JE. Role of thiol-complex formation in 2-hydroxyethyl- methacrylate-induced toxicity in vitro. J Biomed Mater Res A 2011;96:395–401.
[12] Volk J, Engelmann J, Leyhausen G, Geurtsen W. Effects of three resin monomers on the cellular glutathione concentration of cultured human gingival fibroblasts. Dent Mater 2006;22:499–505.
[13] Ma Q. Role of nrf2 in oxidative stress and toxicity. Annu Rev Pharmacol Toxicol 2013;53:401–26.
[14] Chen QM, Maltagliati AJ. Nrf2 at the heart of oxidative stress and cardiac protection. Physiol Genomics 2018;50:77–97.
[15] Kwak M-K, Itoh K, Yamamoto M, Kensler TW. Enhanced expression of the transcription factor Nrf2 by cancer chemopreventive agents: role of antioxidant response element-like sequences in the nrf2 promoter. Mol Cell Biol 2002;22:2883–92.
[16] Atia A, Alrawaiq N, Abdullah A. A review of NAD(P)H: quinone oxidoreductase 1 (NQO1); a multifunctional antioxidant enzyme. J Appl Pharm Sci 2014;4:118–22.
[17] Chorley BN, Campbell MR, Wang X, Karaca M, Sambandan D, Bangura F, et al. Identification of novel NRF2-regulated genes by ChIP-Seq: influence on retinoid X receptor alpha. Nucleic Acids Res 2012;40:7416–29.
[18] Fukai T, Ushio-Fukai M. Superoxide dismutases: role in redox signaling, vascular function, and diseases. Antioxid Redox Signal 2011;15:1583–606.
[19] Stocker R, Yamamoto Y, Mcdonagh AF, Glazer AN, Ames BN. Bilirubin is an antioxidant of possible physiological importance. Science 1986;235:1043–6.
[20] Vnukov VV, Gutsenko OI, Milyutina NP, Kornienko IV, Ananyan AA, Plotnikov AA, et al. SkQ1 regulates expression of Nrf2, ARE-controlled genes encoding antioxidant enzymes, and their activity in cerebral cortex under oxidative stress. Biochemistry Moscow 2017;82:942–52.
[21] Baker BM, Chen CS. Deconstructing the third dimension: how 3D culture microenvironments alter cellular cues. J Cell Sci 2012;125:3015–24.
[22] Cukierman E, Pankov R, Stevens DS, Yamada KM. Taking cell-matrix adhesions to the third dimension. Science 2001;294:1708–12.
[23] Hillmann G, Gebert A, Geurtsen W. Matrix expression and proliferation of primary gingival fibroblasts in a three dimensional cell culture model. J Cell Sci 1999;112:2823–32.
[24] Baharvand H, Hashemi SM, Ashtiani SK, Farrokhi A. Differentiation of human embryonic stem cells into hepatocytes in 2D and 3D culture systems in vitro. Int J Dev Biol 2006;50:645–52.
[25] Kenny PA, Lee GY, Myers CA, Neve RM, Semeiks JR, Spellman PT, et al. The morphologies of breast cancer cell lines in

three-dimensional assays correlate with their profiles of gene expression. Mol Oncol 2007;1:84–96.
[26] Petrie RJ, Doyle AD, Yamada KM. Random versus directionally persistent cell migration. Nat Rev Mol Cell Biol 2009;10:538–49.
[27] Riedl A, Schlederer M, Pudelko K, Stadler M, Walter S, Unterleuthner D, et al. Comparison of cancer cells in 2D vs 3D culture reveals differences in AKT-mTOR-S6K signaling and drug responses. J Cell Sci 2017;130:203–18.
[28] Zietarska M, Maugard CM, Filali-Mouhim A, Alam-Fahmy M, Tonin PN, Provencher DM, et al. Molecular description of a 3D in vitro model for the study of epithelial ovarian cancer (EOC). Mol Carcinog 2007;46:872–85.
[29] Zschenker O, Streichert T, Hehlgans S, Cordes N. Genome-wide gene expression analysis in cancer cells reveals 3D growth to affect ECM and processes associated with cell adhesion but not DNA repair. PLoS One 2012;7:e34279.
[30] Li M, Rezakhanlou AM, Chavez-Munoz C, Lai A, Ghahary A. Keratinocyte-releasable factors increased the expression of MMP1 and MMP3 in co-cultured fibroblasts under both 2D and 3D culture conditions. Mol Cell Biochem 2009;332:1–8.
[31] Sawicki G, Marcoux Y, Sarkhosh K, Tredget EE, Ghahary A. Interaction of keratinocytes and fibroblasts modulates the expression of matrix metalloproteinases-2 and -9 and their inhibitors. Mol Cell Biochem 2005;269:209–16.
[32] Wang Z, Wang Y, Farhangfar F, Zimmer M, Zhang Y. Enhanced keratinocyte proliferation and migration in co-culture with fibroblasts. PLoS One 2012;7:e40951.
[33] Werner S, Krieg T, Smola H. Keratinocyte-fibroblast interactions in wound healing. J Invest Dermatol 2007;127:998–1008.
[34] Izumi K, Song J, Feinberg SE. Development of a tissue-engineered human oral mucosa: from the bench to the bed side. Cells Tissues Organs 2004;176:134–52.
[35] Buskermolen JK, Reijnders CMA, Spiekstra SW, Steinberg T, Kleverlaan CJ, Feilzer AJ, et al. Development of a full-thickness human gingiva equivalent constructed from immortalized keratinocytes and fibroblasts. Tissue Eng Part C 2016;22:781–91.
[36] Dongari-Bagtzoglou A, Kashleva H. Development of a highly reproducible three-dimensional organotypic model of the oral mucosa. Nat Protoc 2006;1:2012–8.
[37] Claveau I, Mostefaoui Y, Rouabhia M. Basement membrane protein and matrix metalloproteinase deregulation in engineered human oral mucosa following infection with Candida albicans. Matrix Biol 2004;23:477–86.
[38] Mostefaoui Y, Bart C, Frenette M, Rouabhia M. Candida albicans and Streptococcus salivarius modulate IL-6, IL-8, and TNF-alpha expression and secretion by engineered human oral mucosa cells. Cell Microbiol 2004;6:1085–96.
[39] Schmalz G, Arenholt-Bindslev D, Hiller K-A, Schweikl H. Epithelium-fibroblast co-culture for assessing mucosal irritancy of metals used in dentistry. Eur J Oral Sci 1997;105:86–91.
[40] Rheinwald JG, Hahn WC, Ramsey MR, Wu JY, Guo Z, Tsao H, et al. A two-stage, p16INK4A- and p53-dependent keratinocyte senescence mechanism that limits replicative potential independent of telomere status. Mol Cell Biol 2002;22:5157–72.
[41] Ruijter JM, Ramakers C, Hoogaars WMH, Karlen Y, Bakker O, Van den Hoff MJB, et al. Amplification efficiency: linking baseline and bias in the analysis of quantitative PCR data. Nucleic Acids Res 2009;37:e45.
[42] Vandesompele J, De Preter K, Pattyn F, Poppe B, Van Roy N, De Paepe A, et al. Accurate normalization of real-time quantitative RT-PCR data by geometric averaging of multiple internal control genes. Genome Biol 2002;3:1–11.
[43] Perduns R, Volk J, Schertl P, Leyhausen G, Geurtsen W. HEMA modulates the transcription of genes related to oxidative defense, inflammatory response and organization of the ECM in human oral cells. Dent Mater 2019;35:501–10.
[44] Schertl P, Volk J, Perduns R, Adam K, Leyhausen G, Bakopoulou A, et al. Impaired angiogenic differentiation of dental pulp stem cells during exposure to the resinous monomer triethylene glycol dimethacrylate. Dent Mater 2019;35:144–55.
[45] Pfaffl MW. A new mathematical model for relative quantification in real-time RT-PCR. Nucleic Acids Res 2001;29:e45.
[46] Catalioto R-M, Festa C, Triolo A, Altamura M, Maggi CA, Giuliani S. Differential effect of ethanol and hydrogen peroxide on barrier function and prostaglandin E2 release in differentiated Caco-2 cells: selective prevention by growth factors. J Pharm Sci 2009;98:713–27.
[47] Krouwer VJD, Hekking LHP, Langelaar-Makkinje M, Regan-Klapisz E, Post JA. Endothelial cell senescence is associated with disrupted cell-cell junctions and increased monolayer permeability. Vasc Cell 2012;4:12.
[48] Kural MH, Billiar KL. Regulating tension in three-dimensional culture environments. Exp Cell Res 2013;319:2447–59.
[49] Ehrlich HP, Hunt TK. Collagen organization critical role in wound contraction. Adv Wound Care (New Rochelle) 2012;1:3–9.
[50] Brown RA, Prajapati R, McGrouther DA, Yannas IV, Eastwood M. Tensional homeostasis in dermal fibroblasts: mechanical responses to mechanical loading in three-dimensional substrates. J Cell Physiol 1998;175:323–32.
[51] Petroll WM, Vishwanath M, Ma L. Corneal fibroblasts respond rapidly to changes in local mechanical stress. Invest Ophthalmol Vis Sci 2004;45:3466–74.
[52] Doyle AD, Carvajal N, Jin A, Matsumoto K, Yamada KM. Local 3D matrix microenvironment regulates cell migration through spatiotemporal dynamics of contractility-dependent adhesions. Nat Commun 2015;6:8720.
[53] Wu P-H, Giri A, Sun SX, Wirtz D. Three-dimensional cell migration does not follow a random walk. Proc Natl Acad Sci U S A 2014;111:3949–54.
[54] Wu P-H, Gilkes DM, Wirtz D. The biophysics of 3D cell migration. Annu Rev Biophys 2018;47:549–67.
[55] Gerzina TM, Hume WR. Diffusion of monomers from bonding resin-resin composite combinations through dentine in vitro. J Dent 1996;24:125–8.
[56] Lanza CRM, De Souza Costa CA, Furlan M, Alécio A, Hebling J. Transdentinal diffusion and cytotoxicity of self-etching adhesive systems. Cell Biol Toxicol 2009;25:533–43.
[57] Viñuela-Prieto JM, Sánchez-Quevedo MC, Alfonso-Rodríguez CA, Oliveira AC, Scionti G, Martín-Piedra MA, et al. Sequential keratinocytic differentiation and maturation in a three-dimensional model of human artificial oral mucosa. J Periodont Res 2015;50:658–65.
[58] Durner J, Walther UI, Zaspel J, Hickel R, Reichl F-X. Metabolism of TEGDMA and HEMA in human cells. Biomaterials 2010;31:818–23.
[59] Nocca G, Ragno R, Carbone V, Martorana GE, Rossetti DV, Gambarini G, et al. Identification of glutathione-methacrylates adducts in gingival fibroblasts and erythrocytes by HPLC-MS and capillary electrophoresis. Dent Mater 2011;27:e87–98.
[60] Sandberg E, Dahlgren UI. Application of HEMA on intact mouse skin-effects on the immune system. Contact Derm 2006;54:186–91.

[61] Sandberg E, Bergenholtz G, Kahu H, Dahlgren UI. Low HEMA conjugation induces high autoantibody titer in mice. J Dent Res 2005;84:537–41.
[62] Savaskan NE, Ufer C, Kühn H, Borchert A. Molecular biology of glutathione peroxidase 4: from genomic structure to developmental expression and neural function. Biol Chem 2007;388:1007–17.
[63] Pederson TC, Aust SD. The role of superoxide and singlet oxygen in lipid peroxidation promoted by xanthine oxidase. Biochem Biophys Res Commun 1973;52:1071–8.
[64] Jansen T, Daiber A. Direct antioxidant properties of bilirubin and biliverdin. Is there a role for biliverdin reductase? Front Pharmacol 2012;3:30.
[65] Kaur H, Hughes MN, Green CJ, Naughton P, Foresti R, Motterlini R. Interaction of bilirubin and biliverdin with reactive nitrogen species. FEBS Letters 2003;543:113–9.
[66] Yeligar SM, Machida K, Kalra VK. Ethanol-induced HO-1 and NQO1 are differentially regulated by HIF-1alpha and Nrf2 to attenuate inflammatory cytokine expression. J Biol Chem 2010;285:35359–73.
[67] Milani P, Gagliardi S, Cova E, Cereda C. SOD1 transcriptional and posttranscriptional regulation and its potential implications in ALS. Neurol Res Int 2011;2011:458427.
[68] Yue X, Lukowski JK, Weaver EM, Skube SB, Hummon AB. Quantitative proteomic and phosphoproteomic comparison of 2D and 3D colon cancer cell culture models. J Proteome Res 2016;15:4265–76.
[69] Jarkovska K, Dvorankova B, Halada P, Kodet O, Szabo P, Gadher SJ, et al. Revelation of fibroblast protein commonalities and differences and their possible roles in wound healing and tumourigenesis using co-culture models of cells. Biol Cell 2014;106:203–18.